

Astrophysics, Year IV
4C00 Msci final project,
Project homepage: <http://www.hep.ucl.ac.uk/~fz/>
Supervisor: Prof. D. J. Miller
Co-Supervisor: Dr. S. T. Boogert
Wednesday, 02 April 2003

Report: Investigation of e+e- Luminosity Spectrum

Firas Zenie,
UCL-HEP

Abstract

This project aims to contribute to a full simulation of the TESLA linear collider, by examining the different reconstruction methods for the luminosity spectrum^{[1][2]}, and their implications for top quark precision mass measurements.

Luminosity spectra are fully simulated by firstly evaluating beam-beam effects using a modified version of guinea-pig^[3], and then simulating bhabha scattering and other QED cross sections using bhwide^[4].

We find that one of the reconstruction methods yields useful results in the case of wide scattering angles (100 to 300 mrad), when one photon or less is emitted in the collision. The reconstruction is also enhanced when the momentum loss correlation between the beams is artificially removed.

Table of Contents

1. Physics Background	3
1.1 Linear Accelerators.....	3
1.1.1 Physics in a TeV linear Collider.....	3
1.1.2 TESLA	4
1.2 e+e- Luminosity spectrum.....	4
1.2.1 Beams spread.....	4
1.2.2 beamstrahlung.....	5
1.2.3 Initial State radiation.....	5
1.3 Reconstruction using Acollinearity and Bhabha scattering.....	5
1.3.1 Frary Miller reconstruction[2].....	5
1.3.2 K Mönig reconstruction[1].....	6
2 Results	6
2.1 General Method.....	6
2.2 Guinea-pig[13],[17],[3].....	6
2.3 Circe[18].....	7
2.4 Bhwide[4].....	7
2.5 First results from Guinea-Pig.....	8
2.6 Early-late energy correlation.....	9
2.6.1 Z-position.....	10
2.7 Luminosity spectra.....	11
2.7.1 Curve Fitting methods.....	12
2.8 Corrections methods.....	13
2.8.1 Filtering angles.....	13
2.8.2 Number of photons radiated.....	14
2.8.3 Correlated dispersion.....	14
2.9 Effect on top cross section.....	14
2.9.1 Top cross section function.....	14
2.9.2 Smearing with the luminosity spectrum.....	15
2.10 Discussion.....	17
3 Conclusion	18
4 References	19
5 Appendix A: The project	20
5.1 Aims fulfillment.....	20
5.2 Main difficulties.....	20
6 Appendix B: Bhabha Kinematics	21
7 Appendix C: $\sqrt{p_1 p_2}$ vs $p_1 + p_2$ as expressions of energy	22

1. Physics Background

1.1 Linear Accelerators

Since the 1960s, most particle accelerators built accelerated particles along a closed, roughly circular path. This is a good design technique, as, firstly it allows to focus the particle and anti-particles using the same magnets; secondly the particles can be made to go round the accelerator several times to attain very high energies, and thirdly the beams can be made to cross several times, to obtain a maximal number of collisions.^[5]

But this design is limited by brehmsstrahlung radiation, the process by which a charged particle radiates a photon when its path is bent—which is nearly constant in a ring-shaped particle accelerator. The amount of emitted brehmsstrahlung is inversely proportional to the mass of the particles —so light particles such as electrons (e^-), positrons (e^+) and muons(μ) are much more affected. LEP(Large Electron-Positron collider), at 60GeV, attained a limit for electrons-positrons, after which the particles loose too much energy in each turn.

The only way to accelerate e^+ and e^- at significantly higher energy appears to be the construction of linear colliders, where particles are accelerated along a linear path.

1.1.1 Physics in a TeV linear Collider

There are several compelling arguments^[6] for building a linear collider with energy range $\sim 100\text{GeV}$ to 1TeV in the next few years. This is the timescale which will see the construction of the LHC (Large Hadron Collider) at CERN in the LEP tunnel, which will attain energies of $\sim 14\text{TeV}$. The main aim for both a linear collider and the LHC is to find the mechanism which gives mass to gauge bosons and fermions, conjectured in the standard model to be the Higgs boson.

At the energies in question, the LHC will suffer from large backgrounds in Higgs production processes, as a consequence of being a hadron collider. This experimental difficulty will make the measurements of Higgs quark couplings, and Higgs self-couplings difficult. Electrons and positrons, as point-like particles, give a much cleaner signal, enabling the direct measurement of Higgs quantum numbers, and of its finer characteristics and threshold (the only parameter not predicted by the standard model is its mass, hints of which have been detected at LEP between 144 and $\sim 200\text{ GeV}$.) It is expected that a Higgs boson could be produced with only 2-3 other products in a linear e^+e^- collider, as opposed to numbers of the order of 100 in LHC.

In effect, the role of an e^+e^- collider is complementary to that of a hadron collider, as LEP has proved, enabling for example the in-depth investigation of W and Z bosons; as such, the building of a linear collider in the same time as LHC would give a complete toolset for particle physics in the next decade.

Beyond the standard model, super symmetry (SUSY) theories predict the existence of supersymmetric *sparticles*, mirroring particles in supersymmetric space and time dimensions. Effects are predicted in the 100-1000GeV range, either directly from sparticles of in this mass range, or indirectly from heavier particles; linear collider measurements could give information to select good SUSY theories.

As part of its programme, and particularly relevant for this project, a linear collider would be used for top quark physics (precise measurement of all top quark parameters), and W and Z boson precision measurements.

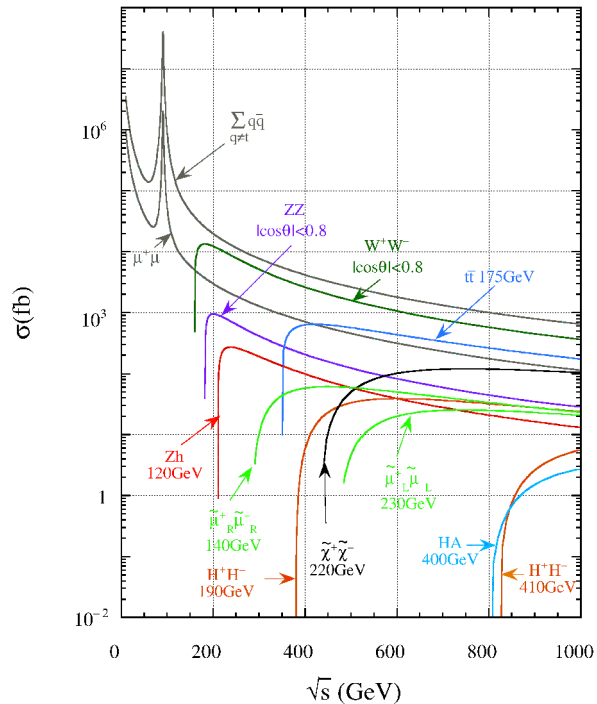


Fig a: Interesting cross sections at a 1TeV linear Collider [7]

1.1.2 TESLA

This project is mainly intended as a study for TESLA the next generation linear accelerator planned in DESY, Hamburg. TESLA (Tera-electron volt Energy Superconducting Linear Accelerator), is one of the contenders for a next generation linear collider. The main others are NLC (Next Linear Collider, Stanford^[8]), JLC (Japan^[7]) and in the longer term, CLIC at CERN^[9](at a higher 3-5 TeV energy range.)

TESLA is planned to accelerate electrons and positrons to a center of mass energy of 500GeV at first. In a second phase, energies of 800GeV-1TeV will be attained. The setup is over 30km in length, and the acceleration is carried out using superconducting niobium RF cavities, cooled at 2K by liquid helium. These allow very high acceleration gradients (more than 30MV/m), and allow the acceleration and conservation of very small bunches.

A major challenge of TESLA is to produce high-luminosity beams: this means achieving very small spot sizes by concentrating the particles into bunches of length of a few hundred μm , and of widths one thousand times less. The bunch populations would average 10^{10} particles, and the bunches have to be damped to reduce emittance in large damping rings, as in fig. b. opposite.

In addition to e^+e^- collisions, TESLA has the capability of colliding e^-e^- (which can be used to search for heavy Majorana neutrinos), as well as γe^- and $\gamma\gamma$ photon collisions, which would test fundamental QCD predictions of the F_2' photon structure function.

1.2 e^+e^- Luminosity spectrum

The type of experiments that are to be carried out at TESLA demand high precision in the knowledge of the luminosity of the beam; unlike the case of LHC, the center of mass energy of a collision cannot be assumed to be twice the beam energy.

In practice, when the beam is run at given energy, some particles lose energy before the collision for several reasons. The range of collision energies is distributed in a spectrum, sharply peaked, with more than 65% of events with 0.1% of nominal energy: this distribution is referred to as the e^+e^- luminosity spectrum, $\partial L/\partial\sqrt{s}$.

It is hoped that by using physics processes known as bhabha scattering, the energy spectrum can be reconstructed with an accuracy of 0.1%. This would be sufficient for top quark physics, whereas investigation of W mass would require an accuracy better by an order of magnitude: 0.01% in the luminosity spectrum.^{[11],[12]}

The three main processes that contribute to an energy loss are machine beamsread, beamstrahlung, and Initial State Radiation. They are detailed below:

1.2.1 Beamsread

This is the smallest source of energy loss. It is induced by the intrinsic energy spread of the e^- and e^+ produced by the machine, and it is an inescapable process.

Because of the process by which the electrons are used to produce the positrons, the latter will have a lower machine energy spread. The value for the positrons is 0.05%, and for the electrons it is 0.15%. This effect is unlikely to be gaussian.

We can already see the difficulty in reconstructing a spectrum to 0.1% accuracy, when the electrons have an intrinsic 0.15% energy spread.

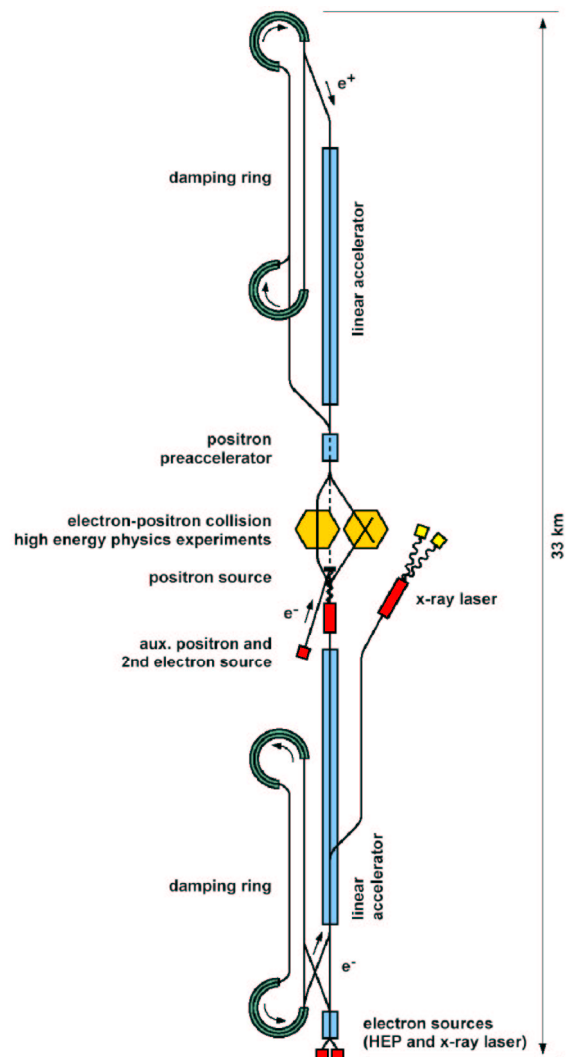


Fig b: TESLA overall layout sketch, [10], II-7.

1.2.2 beamstrahlung

beamstrahlung is the name of the energy loss that electrons and positrons experience when the particles of one beam interact with the electromagnetic field of the opposite bunch. It is equivalent to brehmsstrahlung, which is caused by bending the trajectory of a charged particle, and has the same spectrum; in effect they are both caused by accelerating the particle.^[13]

This is quite a large effect in an accelerator like TESLA^[14], as charges in the bunches are very concentrated due to small beam sizes.

1.2.3 Initial State radiation

Initial State Radiation (ISR) is a consequence of QED. At any given time, one of the beam particles can radiate a photon, thus losing energy.

It can be calculated to great accuracy, and would not need to be measured if it were the only effect present. To calculate it, some QCD cross sections have to be taken into account; we used BHWIDE, a wide angle bhabha scattering simulation program (first developed in LEP^[4].)

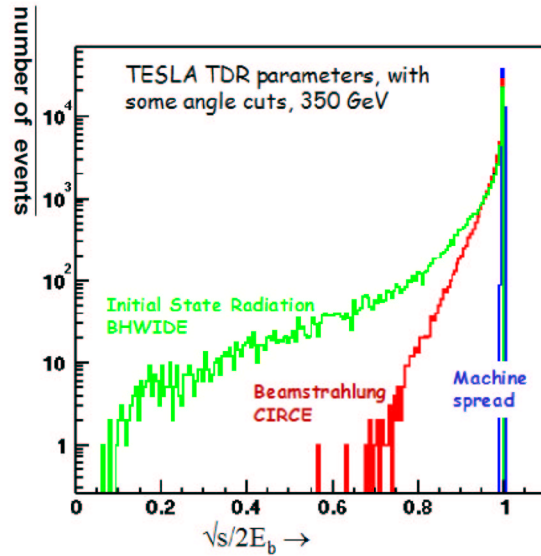


Fig c: plot showing the relative energy losses due to the three main processes^[12].

1.3 Reconstruction using Acollinearity and Bhabha scattering

To regain the accuracy lost from luminosity spectrum smearing in a e^+e^- collider, several methods are considered, using bhabha scattering events. In both cases, for a given event where a photon was radiated the true center of mass energy of the event, \sqrt{s} , can be estimated by measuring the deflection angles of the electron and positron from the beam axis. It has been shown that the most straightforward approach is to use the particles scattered between 0.1 and 0.3 radians. At those angles, the reconstruction can be accomplished using the the forward tracking detector, which has high angular accuracy, and helped by calorimeter endcap for the lower energy events.

The reasons why this is the preferred process to estimate \sqrt{s} are that it has better statistics than the physics channels (400 times the $\mu\mu$ rate in our angular range), and it has a good energy resolution. At small angles, the error on \sqrt{s} grows, becoming more significant below 0.1 radians.

The process is basically described by the exchange of a virtual photon, or a Z^0 boson. In our angular range, the s-channel dominates, and the Z^0 contribution is small.^[15]

From outgoing particle angles the momentum loss can be estimated, and thus the energy loss from nominal energy, under the assumptions that a.) only one photon has been radiated and b.) it was radiated along the beam.

The distribution of \sqrt{s} will then give the luminosity spectrum, $\partial L / \partial \sqrt{s}$.

Two methods have been considered in the course of the project:

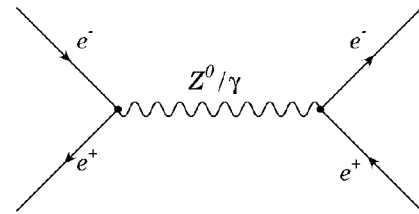


Fig d: s-channel bhabha scattering

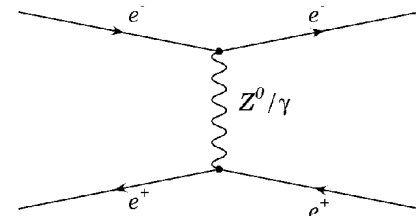


Fig e: t-channel bhabha scattering

1.3.1 Frary Miller reconstruction^[2]

The angles θ_1 and θ_2 are defined as shown in fig. f. The acollinearity angle θ_A is equal to the difference of θ_1 and θ_2 ($\theta_A = \theta_1 - \theta_2$).

The angle θ is taken as the average between θ_1 and θ_2 . For small acollinearity ($\theta_A \ll \theta$), we have $\theta_A = (\Delta p / p_b) \sin \theta$, where $\Delta p = p_1 - p_2$, the momentum difference between the two particles at collision.

The quantity needed is $\sqrt{S} \approx 2p_{nom} - \theta_A p_{nom} / \sin \theta$ by this estimate.

Considering the error: for small θ_A , if the error is Gaussian, $\sigma_{\sqrt{S}} \approx \sigma_{\Delta p} \approx \sigma_{\theta_A} p_b / \sin \theta \approx \sqrt{\sigma_{pb}}$.

So the error increases as the scattering angle θ approaches 0, which implies better luminosity resolution for slightly larger angles.

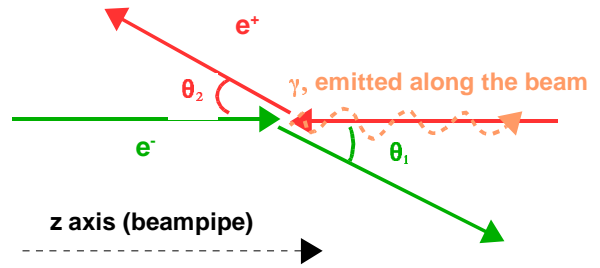


Fig f: bhabha scattering event schematic diagram

1.3.2 K Mönig reconstruction^[1]

This approximation can be derived directly from bhabha scattering kinematics (cf. Appendix B): if the 4-momenta of an electron and a positron are added to find the center of mass energy, and it is assumed that a.) one photon is radiated in the direction of the beam pipe, and b.) the paths are coplanar, then some algebra will yield:

$$\sqrt{s} \approx \sqrt{\cot(\theta_1/2) \cot(\theta_2/2)} \quad \text{cf. Appendix B for algebra.}$$

2 Results

The aim of project was to provide a full simulation of the reconstruction and bhabha events, and this was extended to a qualitative evaluation of the effect of a reconstructed spectrum on the top quark cross section.

2.1 General Method

The general method employed was that of a step through simulation.

First, the beam-beam interaction is simulated using the guinea-pig program. Then the output from guinea-pig is taken as input for the bhwide bhabha scattering simulation.

At all stages of the process, data is outputted and visualised to check for errors: a plot that cannot be explained from physics points either to a bug in the code or to a new physics result.

The programming was divided into writing data visualisation routines using Root^[16] to check the physics, and interfacing the different pieces of software. Scripts were also produced to run the software as a scan over sets of parameters.

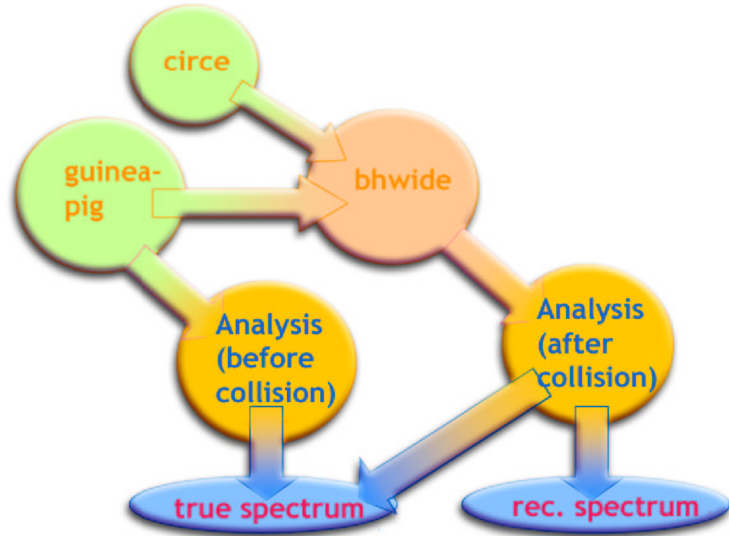


Fig g: flowchart of software used

2.2 Guinea-pig^{[13],[17],[3]}

Guinea pig was written by D. Schulte in 1997, and models beam-beam interactions in next-generation linear colliders. Its approach is to treat the bunch as a relativistic ionised fluid, so that the electromagnetic interactions are treated like a plasma. The beams are discretised into a 3-dimensional grid, where each element of the grid is a macro particle. Typically 20,000 to 500,000 macro particles are used; the beams are longitudinally cut into slices that can then be interacted subsequently with each other slice. Because of their relativistic behaviour, the interaction between the slices can be treated as a two-dimensional problem—a macro particle only interacts with macro particles around it in the constant z plane. So

the problem is solved using a "clouds in cells" approach, where the potential from all surrounding cells is evaluated to calculate forces on the macro-particle.

The output files of interest were the files containing macro-particles in the beams before collision, and most importantly the lumi file, which contains pairs of macro particles that are to collide. It is those lumi events that are then fed into the physics simulation program bhwide.

Our version of guinea-pig was modified to output the full 4-momenta of the electron and positron, to enable the accurate calculation of the true spectrum. Modifications were carried out by S. Boogert.

In later runs, the output from many runs of guinea-pig are concatenated, to give a large statistical sample for bhwide to produce events from. Usually, 100 runs were performed in a sequence, giving approximately 10,000 events each.

2.3 Circe^[18]

Circe is a parametrisation of guinea-pig output written by T. Ohl in 1997. It provides a faster way to generate beamstrahlung beam data, and the function it uses as a parametrisation of the spectrum is often used as a fitting function for linear collider luminosity spectra (cf. Ref [1].)

The fitting function used is of the form:

$$f(x) = a_0 \delta(1-x) + a_1 x^{a_2} (1-x)^{a_3} \quad (\text{equ. 1.})$$

where $f(x)$ represents the luminosity spectrum $\partial L / \partial \sqrt{S}$,

x is the $\sqrt{S} / \sqrt{S}_{\text{nominal}}$, the ratio of center of mass energy to beam energy,

and $a_0 \dots a_3$ are the four fitting parameters—one of which is usually be found by normalisation of the spectrum.

2.4 Bhwide^[4]

Bhwide is a wide angle bhabha simulation, originally written for LEP. We use it with input beams from guinea-pig, as it takes into account the most important QCD cross-sections in its calculation of ISR. Guinea-pig has the built in capability to do an ISR calculation, but bhwide was chosen, being a more extensive solution.

We embed bhwide in a home made program ("bhwrn" developed mostly by S. Boogert) so that it accepts inputs from different beam simulations: at runtime, there is the choice of using guinea-pig, circe beams or beams with no energy loss simulation. There are the added options to a.) include/exclude beamsread b.) boost all components of the particles' momenta, as opposed to just the z-component c.)

Bhwide has an intrinsic angle cut: it will only output events where the deflection angle is more than ~ 110 mrad.

In our runs, we typically generated 500,000 to 1 Million events to generate a luminosity spectrum from.

2.5 First results from Guinea-Pig

The first term was almost exclusively dedicated to running the SLAC version of guinea-pig, which is optimised for NLC-B parameters. Several approaches were tried in loading the beam files and displaying information.

These runs mostly served as a check of guinea-pig and of our understanding of its inputs and outputs, as well as a learning platform for scripting and for the root C++ framework used.

Many physical parameters were outputted, to gain visual understanding of the features, for example: energy, angular offsets, spatial coordinates of particles.

Interesting features appear when varying one parameter in a series of runs, for example:

- different centre of mass energies.
- varying the beam offset on the x axis (typically by up to a few hundred nm.)
- varying the beam offset on the y axis (typically by up to 10 nm.)

Two interesting plots are presented below, in figures h and i: we notice how the angular distribution is asymmetric when the beam offsets are varied.

This figure represents different parameters of the positron beam with an x-offset of 50, 100, 150, 200 and 400 nm.

The most interesting pattern to notice is that the angle of the beam to the x-axis (theta-x) has an asymmetric distribution, with two peaks. In the electron beam the distribution is the mirror image of this one. This shows that the beam polarises into two beams, separated from the centre, as its offset increases.

Notice also that the distribution in the y direction becomes more sharply peaked with higher x-offset.

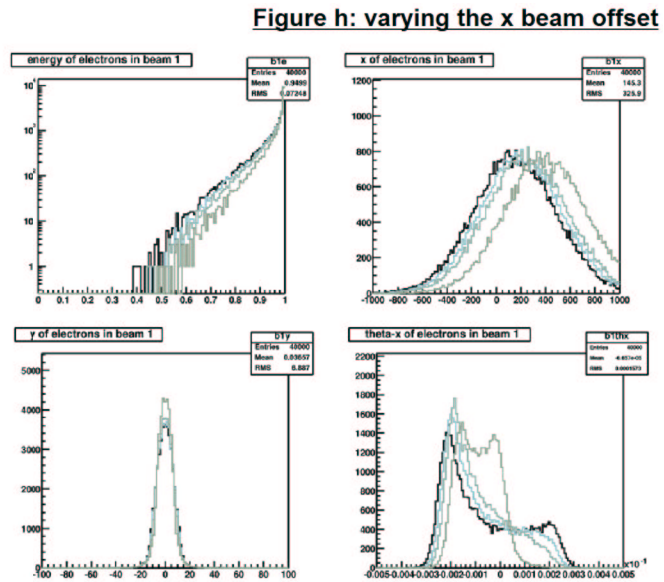
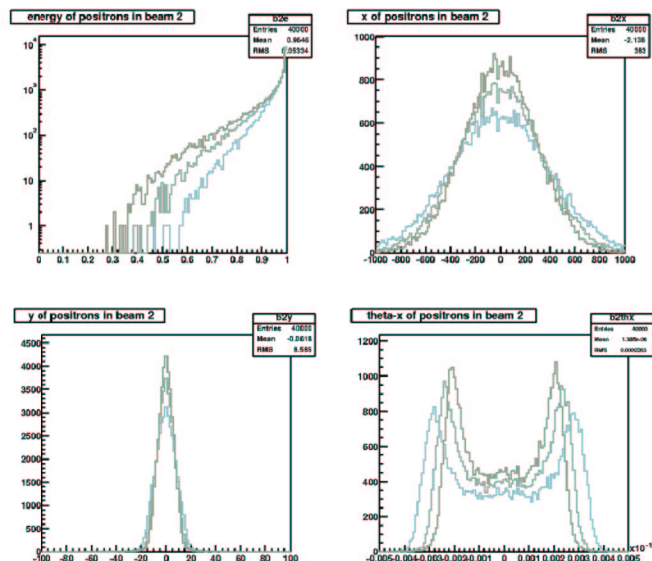


Figure i: varying the beam energy

In this figure the positron beam parameters are plotted with centre of mass energies of 350, 500 and 650 GeV.

The distribution of theta-x (angle to the x-axis) becomes more sharply polarised at higher energies, and the luminosity spectrum widens, due to higher beamstrahlung.

The x and y positions distributions, sharpen at higher energies due to adiabatic damping. Adiabatic damping arises from the particles' relativistic speeds, and causes the transverse offsets of the beam to diminish as $1/\sqrt{\gamma}$, due to the invariance of the normalised emittance (since the $1-\sigma$ beam envelope goes as the square root of the emittance, which has a momentum term.) This means that the beams get more focussed as the particles go faster; it is one of the few processes that increases luminosity with increasing beam energy.



2.6 Early-late energy correlation

Our first new physics result is the identification of a linear correlation between position within the bunch and energy of interaction. Since guinea-pig goes through layers in the bunch in sequential order, we can process an output file directly, and output the energy contained in macro-particles that generate events. Physically, this is understandable as the electron/positron at the end of a bunch has crossed more field through more field, and thus has interacted more than the one at the beginning of a bunch.

Since the guinea-pig algorithm goes through each pair of transverse bunch slices before moving to the next slice, there are several dozens macro particles to process within each slice. For this reason, we average 200 lines of the output file before plotting, thus neglecting the computational artefacts. In figure j below the independent variable, labelled 'T', is effectively the line number/200.

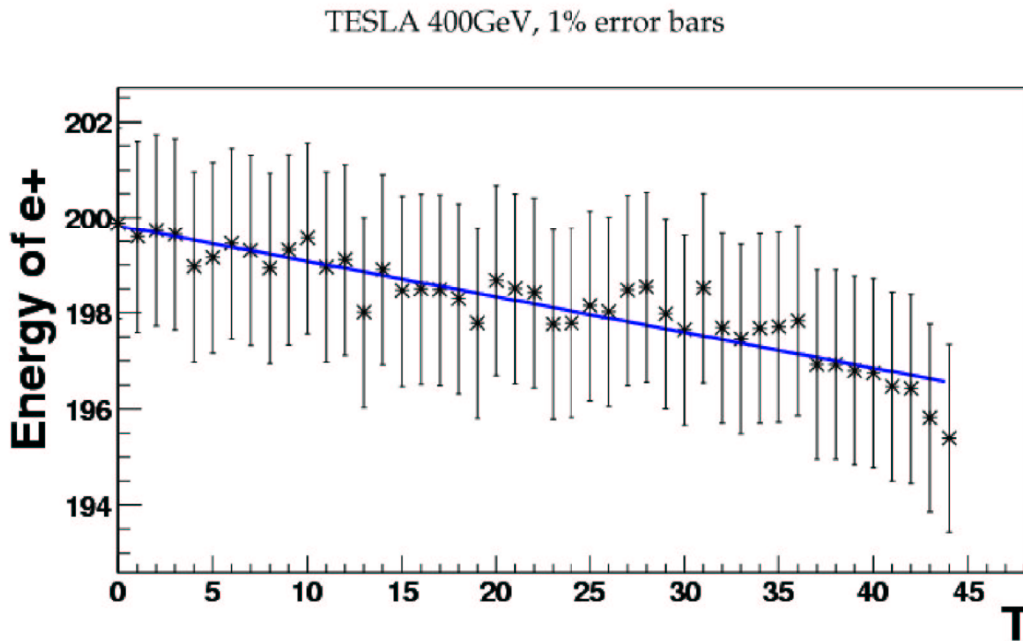
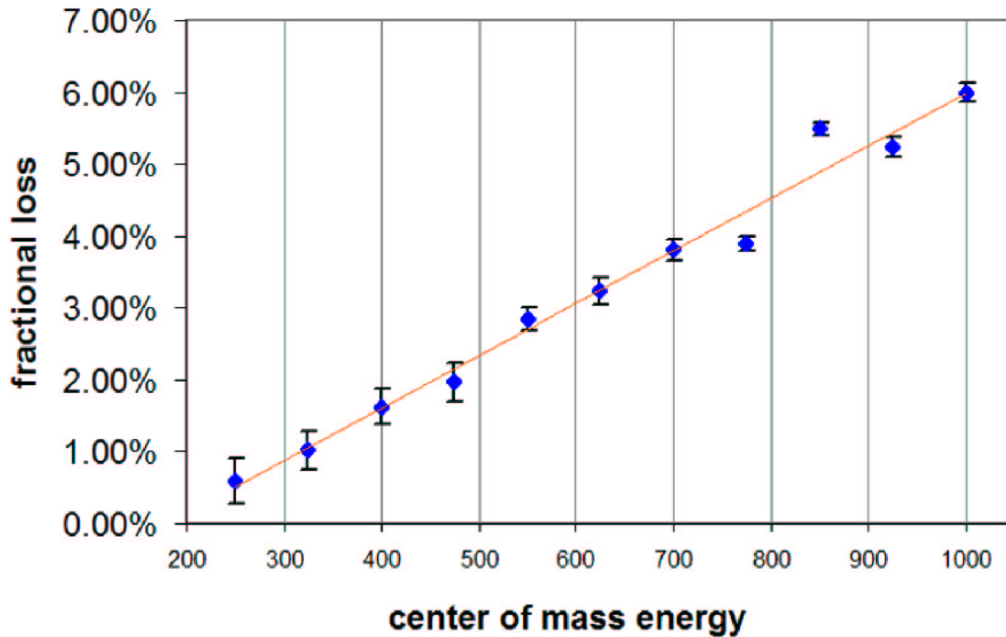


Figure j: plot of collision energy as a function of position in output file

Another interesting quantity is the fractional decrease in energy over a whole bunch, as a function of beam energy. This decrease in energy is found by running guinea-pig at a range of different energies, and finding the scaled energy loss over the range of the fitted linear trendline.

We find another linear relation: at $\sqrt{s}=500\text{GeV}$, average 2.2% energy loss. But at 1TeV, will have lost $\sim 6\%$. This is comparable to values found in literature by independent methods: in ref [1], (p1) the average energy lost for an electron at $\sqrt{s}=500\text{GeV}$ is 1.5%, which is compatible with an average loss of $\sim 2\%$ from an electrons at the beginning of the bunch vs those at the end.

Fig k: fractional energy loss through a whole bunch in TESLA, at varying beam energy:



2.6.1 Z-position

We also plot z-position of electrons around the interaction point, as the software runs through the bunch. As we expect intuitively, at the beginning and the end of the interaction the z-positions of the interacting particles will be less spread, as the bunches are going through each other. Note that the envelope is what is interesting here, rather than the up-down pattern which is a computational effect.

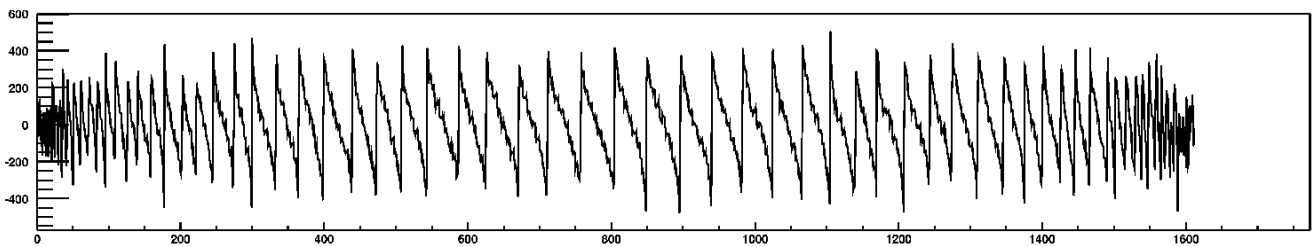


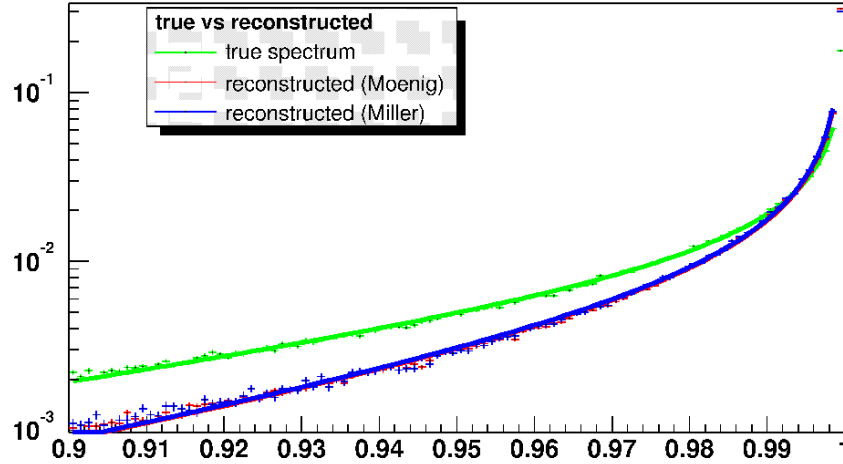
Fig L: plot of z-position vs time

2.7 Luminosity spectra

A full luminosity spectrum can then be produced. The true \sqrt{s} for each event is evaluated from the 4-momenta. The scattering angles are calculated from the dot products of the 3D momenta, and thus we can evaluate \sqrt{s}_{est} , the estimated centre of mass energy. The Luminosity Spectrum, $\partial L / \partial \sqrt{s}$, is the distribution of \sqrt{s} for all events.

The curves are plotted along with the lines of best fit, and the fit parameters, as well as the statistical moments of the curves, are outputted. We only output the curves from 90% of the energy upwards, as below this region the calorimeter has enough resolution to evaluate the centre of mass energy of an event, and the effect of the lower tail of the spectrum is limited, due to the low number of events.

Figure m: full luminosity spectrum, TESLA, 350GeV



Using fitting function $\sqrt{s} \sqrt{s_{\text{nom}}} = ax^2(1-x)^2$:: last bin from integral

true mean: 9.7785E-01
 rec mean: 9.8567E-01
 true rms: 2.5408E-02
 rec rms: 2.1172E-02
 true skew: 4.1717E+03
 rec skew: 4.1709E+03
 true kurt: 3.2880E+05
 rec kurt: 3.2870E+05
 kept 5.0000E+05 points

True Lum Spectrum	Rec Moenig	Rec Miller
fit: $\chi^2 = 1.9154E+02$	fit: $\chi^2 = 3.8232E+02$	fit: $\chi^2 = 2.6214E+02$
a = 1.4698E-03 ± 2.4800E-05	a = 6.9771E-04 ± 1.1754E-05	a = 6.8656E-04 ± 1.6482E-05
b = 1.0013E+01 ± 1.4450E-01	b = 1.3735E+01 ± 1.6186E-01	b = 1.3603E+01 ± 2.3118E-01
c = -5.7802E-01 ± 3.1395E-03	c = -7.2799E-01 ± 3.0253E-03	c = -7.3495E-01 ± 4.3078E-03
last bin = -1.2742E+01 % of area	last bin = 1.8774E+01 % of area	last bin = 1.6632E+01 % of area

2.7.1 Curve Fitting methods

The curve fitting equation is non-standard: it is given by equation 1 above.

We use the in-built Root chi-squared fitting classes.

We find that a convergence can usually never be found if the whole histogram is to be fitted: the $(1-x)^a$ is too sharply peaked at 1, and the dirac delta function then needs a negative coefficient effectively model the peak. After several attempts at using gaussians and exponentials, as well as other mathematical devices to avoid singularities, an empirical method is settled for: the luminosity spectrum histogram is fitted up to the last bin, with a simpler version of equation (1), and the last bin can then be calculated from normalisation (as the area of the spectrum is normalised to 1.)

This has the advantage of giving a very close fit, and of directly giving value of the last bin, which is an important physical quantity (fraction of particles within 0.1% of nominal energy.)

The function we use is of the form:

$$f(x) = \frac{\sqrt{S}}{\sqrt{S_{nom}}} = a x^b (1-x)^c$$

, where a, b and c are fitting parameters, and a 4th parameter d is the value of the last bin, and is obtained from the normalisation of the area under the curve.

2.8 Corrections methods

Two things can be noted about the spectra in figure m: the two reconstructed curves, in red and green, are very close. They are also quite far from the true luminosity spectrum, as they are more sharply peaked: this implies that there is more energy loss than is being accounted for by the reconstruction, as the curves are broader.

Both reconstructions assume the following:

- one photon emitted only
- photon is emitted along the beam axis
- the acolinearity is small
- the outgoing electron and positron angles are in the region $0.1 < \theta < 0.3$
- the outgoing e^+ and e^- are on the same plane

The procedure we apply ourselves to is to look for the conditions that the reconstructions give an accurate fit of the true luminosity spectrum.

2.8.1 Filtering angles

The first step is to apply angle cuts to the standard accelerator spherical coordinates angles.

In all subsequent images, the following angle cuts are applied : $0.1 < \theta_1 < 0.3$, $0.1 < \theta_2 < 0.3$. This is a realistic angle cut for the reconstruction, which would use the forward tracking detector in TESLA.

This is best exemplified in figures n, o below. Notice also the intrinsic bhwide angle cut: no particles are emitted below $\theta = 0.11$ radians even in the uncut phase space in figure n.

Figures n, o: reduction of θ phase space

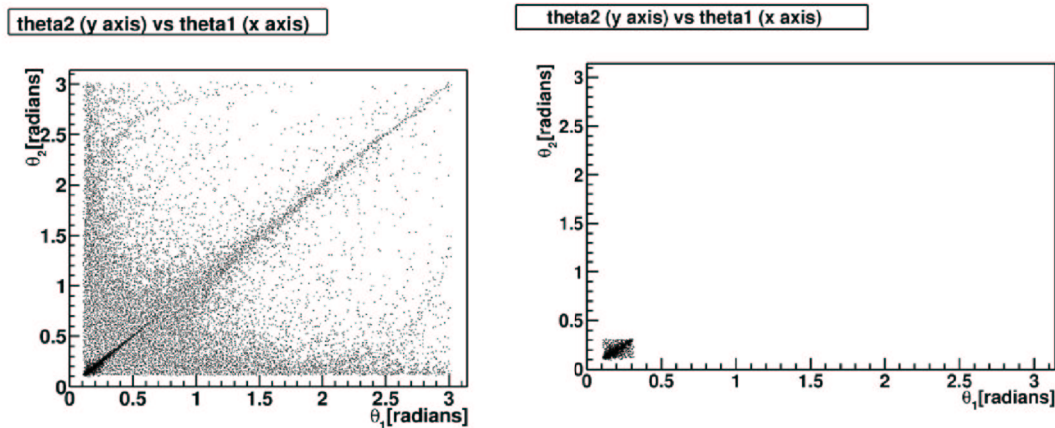


Figure n: θ phase space before angle cuts

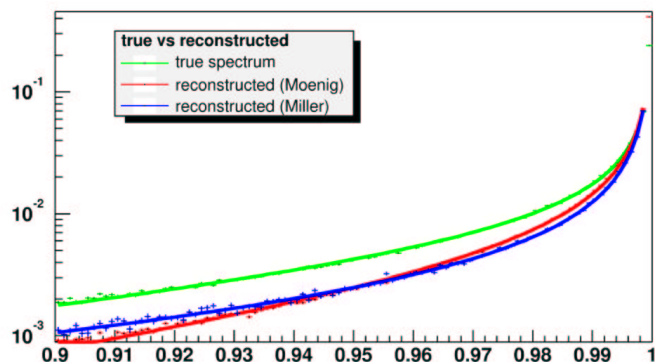
Figure o: θ phase space after angle cuts

Applying angle cuts on theta alone marginally improves the reconstructions, and exposes the difference in reconstruction methods.

We also attempt to restrict the acoplanarity by also filtering out events with a large φ angle difference, but we find that

- a.) the φ_1 and φ_2 angle distributions are random, between $-\pi$ and π and
- b.) the vast majority of events are co-planar, i.e. have the same φ angle.

Figure p: luminosity spectrum with theta angle cuts



2.8.2 Number of photons radiated

The number of radiated photons can be obtained from our modified version of bhwide. We restrict the analysis to events where one or less photons have been emitted. This, if combined with the theta cuts above, dramatically improves the reconstruction, especially that proposed by Frary-Miller, where:

--the proportion of events in the last bin is now found accurately (which is crucial for the top cross section smearing, cf section 2.9.2)

--the reconstruction is good in the region above with energy above 97% of nominal energy, which is precisely that where the calorimeter lacks in resolution.

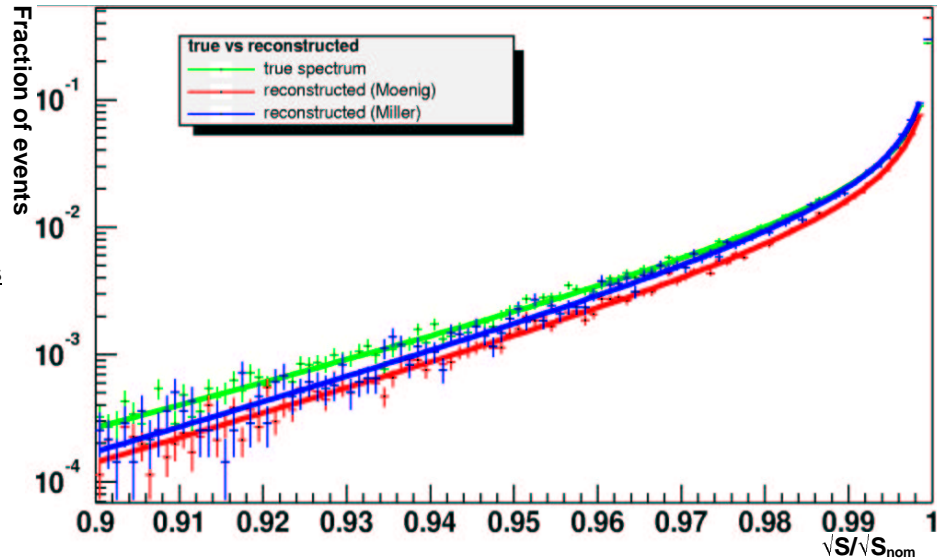


Figure q: luminosity spectrum for events with less than two photons radiated

2.8.3 Correlated dispersion

One of the original questions asked was: "Does correlated momentum loss compensate for momentum mismatch?"

To test this, we artificially 'decorrelate': we force bhwide, the collision program, to choose electrons and positrons from different positions within the beam created by guinea-pig.

Whilst this does not dramatically increase the accuracy of the last bin content, it improves the reconstruction in the region below 97% of nominal energy, which can be subject to calorimeter testing.

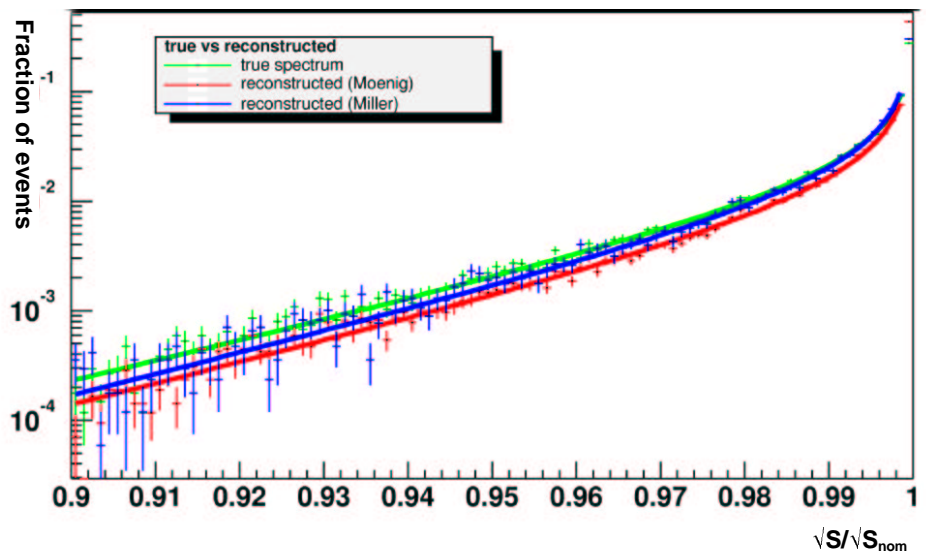


Figure q: luminosity spectrum for events with less than two photons radiated

2.9 Effect on top cross section

We investigate the effect of the luminosity spectrum on the observed top quark production cross section.

2.9.1 Top cross section function

In the absence of a top quark cross section generator, and of a top mass and width fitter, we construct a function that mimics the top cross section, and evaluate the effect on it qualitatively.

The function is of form

$$g : x \rightarrow e^{-x - \sqrt{-\ln(\frac{1}{2})}}$$

$$T : x \rightarrow \begin{cases} g(x), & \text{if } x \leq 0 \\ 1 - g(-x) + \frac{e^{-\frac{x}{2}}}{2}, & \text{if } x > 0 \end{cases}$$

which is an easily computable piece-wise function.

Figure s shows the function plotted "as is."

Figure p shows the function plotted with a shift of 349 GeV, approximately $2m_{top}$. So in practice, we plot:

$$T(x - 2m_{top})$$

taking $2m_{top} = 349$ GeV,

and our function models $\Gamma_{top} \sim 3$.

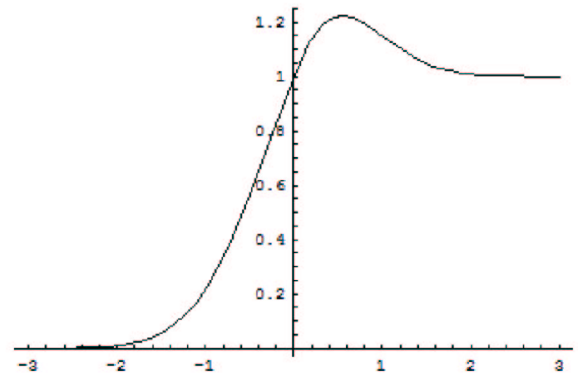


Figure s: top cross section function

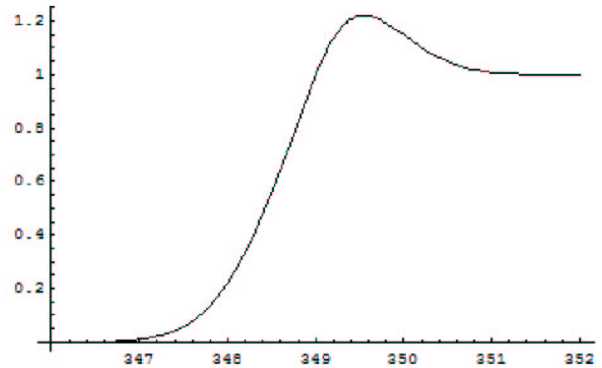


Figure p: top cross section function, as used shifter by $2m_{top} \sim 349$ GeV

2.9.2 Smearing with the luminosity spectrum

To smear the cross section, we treat the luminosity spectrum as a probability distribution, so that at every point, the degraded top cross section is given by:

$$T'(y) = \int_{0.9y}^y T(y') L\left(\frac{y'}{y}\right) dy'$$

where:

$$y = x - 2m_{top}$$

$L(y)$ is the luminosity spectrum

$T(y)$ is the top cross section function

y' an integration variable

This is readily done computationally for every point, and holds mathematically because of the normalisation of the luminosity spectrum.

The same colours are used for the true and reconstructed spectra: in green, the true spectrum. In red, the K. Monig reconstruction method. In blue, the Frary-Miller reconstruction method.

This graph shows that there is a significant difference when the top cross section is degraded by the true and reconstructed spectra.

This is mostly due to the fact that the sharpness of the peak is not reconstructed accurately: so the reconstructed luminosity degrades far less than the true luminosity.

When using events that have only radiated one photon, as in figure u, the cross section degraded by the Frary-Miller reconstructed spectrum is much closer to the true degradation than without the 1 photon cut.

This is due to the accurate prediction of the top bin events.

As mentioned earlier, the de-correlation of events in the bunch does not bring much to the top cross section degradation, as it mostly corrects effects below 97% of \sqrt{s}_{nom} .

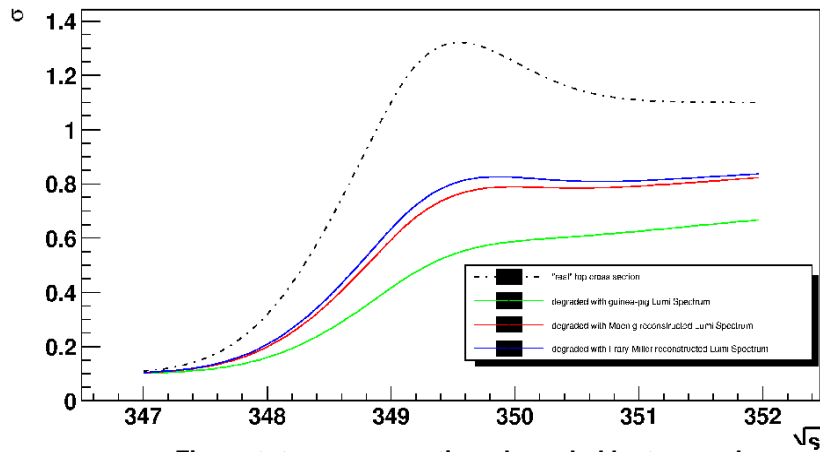


Figure t: top cross section, degraded by true and reconstructed spectra

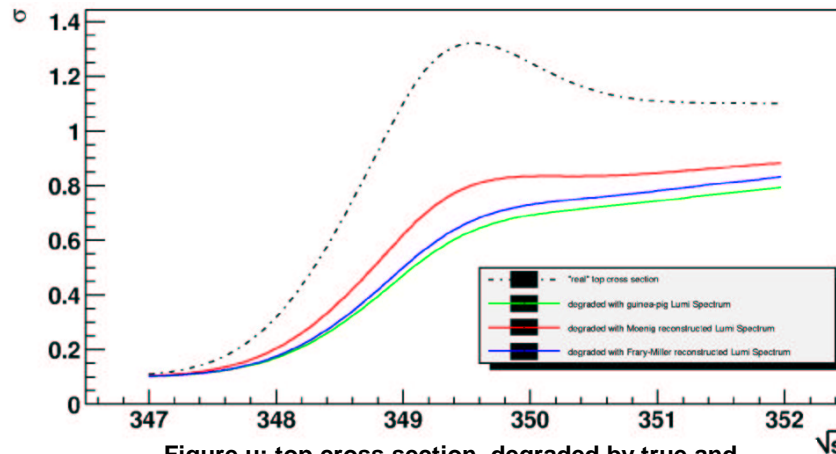


Figure u: top cross section, degraded by true and reconstructed spectra, with 1 photon cut

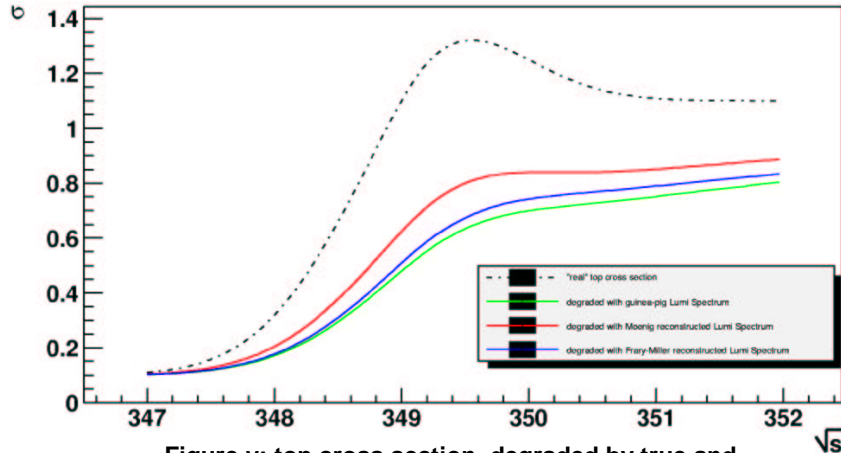


Figure v: top cross section, degraded by true and reconstructed spectra, with 1 photon cut and de-correlation

2.10 Discussion

Filtering events that have radiated only one photon removes what is probably the main cause of discrepancy between the true centre of mass energy of an interaction and that estimated with the Frary-Miller approximation. This is best exemplified by figs w and x: a surface plot where true versus estimated centre of mass energies are plotted as scatter points. In both plots the vast majority of events are in the small area surrounding (1,1). In the unfiltered data plot, there exists a real correlation, but there is also a significant number of reconstructed events that are too low. In the filtered data, it is these events that are filtered out.

The photon cuts improve the reconstruction mostly in the area above 97% of nominal energy: they give a good estimate of the ratio between events in the top 1% and the rest (last bin.) Artificially de-correlating events improves the spectrum below this ~97% limit—but does not significantly improve the accuracy above that limit. Combining these results with endcap calorimeter measurements is probably the solution that will be used.

	True spectrum	Rec. (Miller)	difference
Angle filter only	5.10%	23.70%	18.60%
1 photon filter	26.90%	29.25%	2.35%
decorrelated	27.00%	29.40%	2.44%

The detector question is also an important one: the forward trackers can give a high precision measurement of the angles (~20-39 μ rads in our range), but they are likely to have only 90% efficiency, which is not enough for good luminosity monitoring. However, the whole region is backed by the CALICE calorimeter, which can give 100% efficiency in detecting high-energy electrons. Thus combining the two should probably be done.

To account for the early-late bunch correlation, there is a possibility of using the LCAL small angle calorimeter (5-27 mrad.) This is not adequate for luminosity monitoring due to the angular range, and the errors that this induces, but its background rate may be used in giving a rough bunch-wide luminosity estimate, as well as an early-late correlation correction.

The success of the luminosity spectrum reconstruction can only be thought of in the context of its purpose. For the purpose of extracting the top mass and width from the top cross section, it has been shown that the spectrum needs to be known to 0.1%, or 1 part in 10^{-3} . For the W parameters, an accuracy ten times greater is required. We have progressed in finding limits in which one of the reconstructions gives acceptable results, but work needs to be done in evaluating the exact effect on the top mass and width, to know just how acceptable the reconstruction is for precision measurements. This, and the generation of the theoretical top cross section should be done using a top fitting program. This was not done because of time constraints, as well as the fact that the top fitting program is soon to be released.^[19]

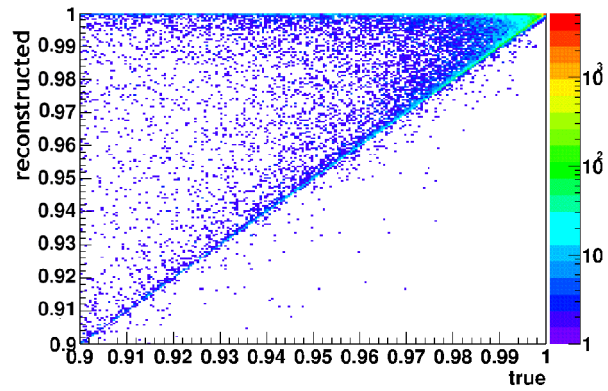


Figure w: true vs estimated center of mass energy, no photon filter

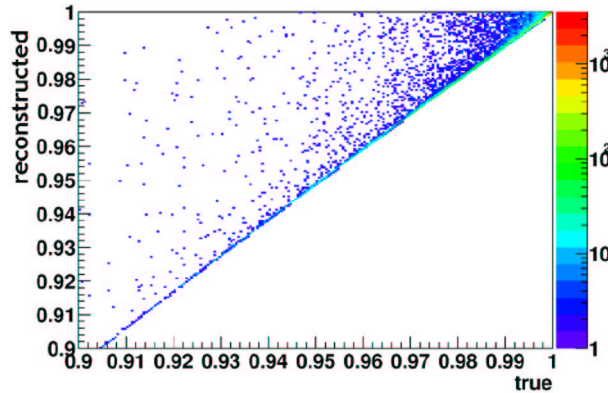


Figure x: true vs estimated center of mass energy, events with less than 2 photons

3 Conclusion

We have progressed in simulating the limits within which the Frary-Miller reconstruction gives acceptable results; most importantly, the number of photons emitted, knowledge of the bunch-bunch energy correlations, and angle cuts. We have also found which parts of the curve are most sensitive to the different parameters.

If it is possible to map these constraints to physical observables in the detectors, a clean centre of mass energy reconstruction can be found on a per-event basis. This will almost certainly also include finding finer causes of discrepancy between the true and reconstructed spectra.

If such observables cannot be found, there is the possibility of reverting to a statistical unfolding of the of the energy loss, whereby the distributions of all sensitive variables are compared and applied to the events.

4 References

- 1: K Mönig, *Measurement of the differential luminosity using bhabha events in the forward-tracking region at TESLA*, 2000 LC-PHSM-2000-60-TESLA
- 2: T Frary, D. J. Miller, *Monitoring the Luminosity Spectrum*, DESY-92-123A p379, 1991, <http://www.hep.ucl.ac.uk/lc/documents/frarymiller.pdf>
- 3: D. Schulte, *Guinea Pig SLAC webpage*, 1997-2002, http://www.sldnt.slac.stanford.edu/nlc/programs/guinea_pig/gp_index.html
- 4: LEP collaboration, software currently hosted University of Tennessee, *BHWIDE, bhabha wide angle scattering simulation tool*, 1990-2003, <http://enigma.phys.utk.edu/>
- 5: D. J. Miller, S.T. Boogert, *Luminosity Monitoring in TESLA*, 2002, Combined contributions to the LCWS workshop, Jeju, Korea
- 6: FishBane, Gaciorowicz, Thornton, *Physics for Scientists and Engineers*, 2000, **pp. 1250-1270**
- 7: Worldwide accelerator study group, *Understanding Matter, Energy, Space and Time: the case for a Linear Collider*, 2003, http://blueox.uoregon.edu/~lc/wwstudy/wwlc_report.html
- 8: JLC collaboration, *JLC homepage*, 1997, <http://www-jlc.kek.jp/>
- 9: NLC collaboration, *Next Linear Collider homepage*, 2003, <http://www-project.slac.stanford.edu/nlc/home.html>
- 10: CLIC collaboration, *Compact Linear Collider homepage*, <http://clicphysics.web.cern.ch/CLICphysics/>
- 11: TESLA collaboration, *TESLA Technical Design Report*, 2001
- 12: D. Cinabro, *Measurement requirements on the luminosity spectrum at a high energy e^+e^- collider*, 2002, LCWS 2002 proceedings, Jeju, Korea
- 13: D. Schulte, *Linear Colliders*, PhD Thesis, 1997
- 14: D. Cinabro, *The tt threshold and machine parameters at the NLC*, 1999, LCWS Sitges proceedings, pp 243, <http://motor1.physics.wayne.edu/~cinabro/nlc/topbeam.ps>
- 15: Montagna, Nicosini, Piccinini, *Precision physics at LEP*, 1998 Rivista del Nuovo Cimento, hep-ph/9802302
- 16: Rene Brun et al., CERN & FNAL, *CERN Root data analysis package framework homepage*, 1994-2003, <http://root.cern.ch>
- 17: D. Schulte, *Beam-beam simulations with guinea-pig*, 1998, International Computational Accelerator Physics Conference, <http://www.slac.stanford.edu/xorg/icap98/papers/F-Th24.pdf>
- 18: T. Ohl, *CIRCE Version 1.0: Beam Spectra for Linear Collider Physics*, 1996 hep-ph/9607454
- 19: A.H. Hoang, A.V. Manohar, I.W. Stewart, T. Teubner, *The Threshold t -bar Cross Section at NNLL Order*, 2002 hep-ph/0107144, Phys.Rev. D

5 Appendix A: The project

5.1 Aims fulfillment

The main aims of the project were to contribute to a complete simulation of the TESLA accelerator, and to examine the reconstruction of the luminosity spectrum, and its behaviour under different circumstances.

Three broad questions were posed in the project proposal:

- a) Does correlated dispersion compensate for disruption?
- b) Is there a correlation with event position within the bunch?
- c) What can we say about offsets and beam bending?

Overall the aims of the project were extended: much time was spent finding the conditions under which the luminosity spectrum reconstructions produce acceptable results, and their effect on top mass measurement.

Questions a.) and b.) were answered satisfactorily, but it is too early at this stage to address question c.). The code written should easily accommodate for beam bending and offsets, as the preliminary guinea-pig plots show, but until problems with the luminosity spectrum are fully understood, it does not seem constructive to investigate exotic beam shapes. Instead of broadening into a methodical taxonomic investigation of beam pathologies, the project was pushed forward to investigate a simple model of the top cross-section, and the influence of the reconstruction on it.

5.2 Main difficulties

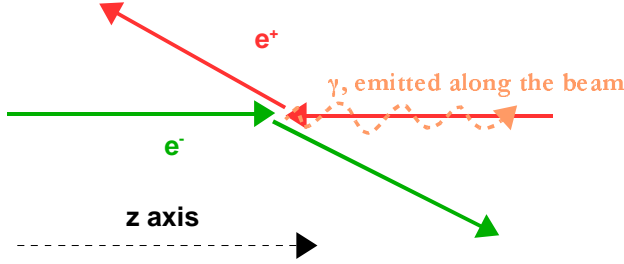
The main difficulties encountered were technical: the codebase is now in 4 languages (c++/ CERN root macros, python, fortran, as well as some linux bash shell), and the author alone wrote ~4000 lines of code. This means that bugs were harder to find, and languages had to be learnt on the spot. For example we had a bug in the boost code in bhwrun, that took weeks to find: this meant data that had been worked on was often rendered useless, and had to be replaced.

Our approach to discovering bugs was mostly through the physics: scatter and surface plots of all aspects of the data were generated, and its physical significance analysed. An unexpected phenomenon would then mean either new physics or buddy code.

A difficult bug was, for example, an asymmetry in the acollinearity angle distribution, which came from the bhwide extension which calculated the boost for the particles. When we discovered it, we did not know whether it came from guinea-pig, bhwide, the interfacing scripts, or indeed the physics.

6 Appendix B: Bhabha Kinematics

We consider the four vectors of the following interaction:



Consider the the four momenta of the electron and positron, before and after the collision.

We can solve all the following algebraic equations using Mathematica(TM).

From momentum conservation, we should have:

$$\bar{p}_{1i} + \bar{p}_{2i} = \bar{p}_{1f} + \bar{p}_{2f} + \bar{p}_\gamma \quad (*)$$

where the \bar{p}_1 and \bar{p}_2 refer to the electron and positron 4-momenta, and the subscripts i and f refer to their initial and final states.

We can also write:

$$\bar{p}_{1i} = \begin{pmatrix} 0 \\ 0 \\ e \\ e \end{pmatrix}, \bar{p}_{2i} = \begin{pmatrix} 0 \\ 0 \\ -e \\ e \end{pmatrix}, \text{ the initial states}$$

$$\bar{p}_{1f} = \begin{pmatrix} p_{1i} \sin \theta_1 \sin \phi_1 \\ p_{1i} \sin \theta_1 \cos \phi_1 \\ p_{1i} \cos \theta_1 \\ p_{1i} \end{pmatrix}, \bar{p}_{2f} = \begin{pmatrix} p_{2i} \sin \theta_2 \sin \phi_2 \\ p_{2i} \sin \theta_2 \cos \phi_2 \\ p_{2i} \cos \theta_2 \\ p_{2i} \end{pmatrix}, \bar{p}_\gamma = \begin{pmatrix} 0 \\ 0 \\ p_\gamma \\ p_\gamma \end{pmatrix}, \text{ the final states}$$

for the initial states, and the final states deflected at arbitrary angles θ and φ ; the photon final momentum is in the z direction, along the axis.

Solving the vector equation (*) above, set $\phi_1 = 0$, $\phi_2 = \pi$ (the interaction is coplanar.)

If we further set the squared center of mass energy, $S = |p_1 + p_2|^2$,

and divide by the nominal energy $S_{nom} = \sqrt{p_1 p_2}$

we get the result:

$$\frac{\sqrt{S}}{\sqrt{S_{nom}}} = \sqrt{\cot \frac{\theta_1}{2} \cot \frac{\theta_2}{2}}, \text{ which is algebraically equivalent to the result quoted by K. Mönig in ref [1]:}$$

$$\frac{\sqrt{S}}{\sqrt{S_{nom}}} = \sqrt{1 - \frac{2 \sin(\theta_1 + \theta_2)}{-\sin \theta_1 - \sin \theta_2 + \sin \theta_1 + \theta_2}}$$

7. Appendix C: $\sqrt{p_1 p_2}$ vs $p_1 + p_2$ as expressions of energy

Before modifying guinea-pig so that all four components of the electrons' and positrons' momenta were available, several approaches were tried to analyse statistical correlations involving the z-magnitudes of the momenta: the sum of the momenta, Σp , and the momentum loss, Δp . These relied on the fact that the outgoing particles are nearly collinear.

An estimate of the true centre of mass energy can be obtained by saying

$$\sqrt{S_{est}} = 2p_{nominal} - \Delta p$$

$$\sqrt{S_{true}} = p_1 + p_2$$

As often, $p_1 + p_2$ is used as an approximation for the centre of mass energy; but we find that this leads to a small offset in at low energies: it is preferable to use $\sqrt{p_1 p_2}$ as an estimate for \sqrt{S} (as, by definition, $S = 2p_1 p_2 - 2\mathbf{p}_1 \cdot \mathbf{p}_2$ and the 3-vector dot product can be neglected due to small angle.)